Vortex model for control of diffuser pressure recovery

Brianno D. Coller
Department of Mechanical Engineering
University of Illinois at Chicago
Chicago, IL 60607-7022
coller@uic.edu

Abstract

The paper outlines an effort to develop moderate dimensional computational models of the shear instability and subsequent highly nonlinear vortex dynamics that occur in a planar diffuser. The ultimate goal is to use the model for testing and synthesis of a non-traditional approach to control that works by triggering instabilities rather than suppressing them. The models appear to capture many of the essential dynamical features, although quantitative discrepancies still need to be resolved.

1 Introduction & Scope

A diffuser is an expanding section of a flow-carrying duct (See Figure 1a). Its purpose is to slow the mean flow in a smooth manner so that kinetic energy of the flow is converted to potential energy manifested in pressure rise. Except for moderate expansion angles (often well under 10°), though, the flow tends to separate from the diffuser wall, shearing the flow into balled-up vortex structures (Figure 1b) that evolve erratically, churning and reversing the flow at times. Figure 1c shows a photo from Coller *et al.* [3] of a physical experiment in which smoke wire flow visualization clearly shows the structures. The process generates great losses and dramatically diminishes the diffuser's ability to raise the pressure of the flow.

The dynamics one observes are the result of a shear instability followed by highly nonlinear fluid interactions. They are similar to phenomena observed in flow separation from general bluff bodies, and aeroelastic flutter instabilities. While the most desirable control objective is to completely re-attach and re-laminarize the flow as shown in Figure 1a, the traditional control paradigm of attempting to stabilize a system or attenuate fluctuations has proven to be exceedingly challenging. Most traditional efforts tend to require overwhelming control authority, unrealistic sensing and actuation abilities, computational power that far surpasses current and near future technologies, and/or require assumptions that the systebe naturally stable or just slightly

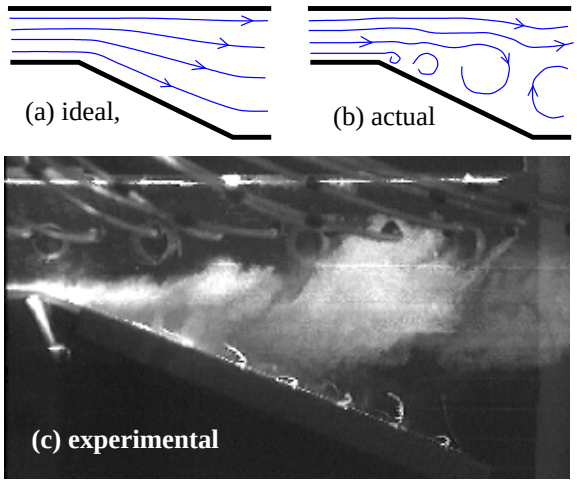

Figure 1: *The planar diffuser. Cartoons of ideal and actual flow are presented in (a) and (b) respectively. A photo of an experiment is shown (c) in which smoke is introduced into the boundary layer.*

unstable. In more practical traditional efforts such as those performed by Kwong and Dowling [12], the researchers are able to reduce peak fluctuations by 7% and spectrum power by 38% with small amplitude blowing and suction from the diffuser lip. However, dispite these favorable indicators, the controller had no effect on pressure recovery.

Encouraging results, though, have recently been flowing from the fluid mechanics community. Researchers [14, 15, 17, 23, 16] have proposed simple open loop control strategies for the diffuser by which *small* sinusoidal forcing is applied near the lip of the expansion either via mechanically actuating a small flap or by blowing and sucking fluid through a narrow slot, imparting momentum perturbations on the order of 10^{-4} to 10^{-3} of that of the nominal flow. For appropriately chosen actuation frequencies, pressure recovery is dramatically improved, at times approaching the maximum theoretically possible [15].

The approach does not work by stabilization and at-

tenuation of fluctuations. Instead, instabilities are triggered in effort to favor large vortex structures that undergo complex interactions and evolve into configurations that favor the physics of pressure recovery. Unfortunately, the control synthesis process occurs via ad-hoc, laborious trial and error. Some of the better controllers stumbled upon are not simple sinusoids and are not intuitively obvious [18].

Herein, we outline the development of a moderate dimensional computational model to capture the essential natural dynamical features of the system, and its response to actuator inputs.

2 Modeling

We implement a 2-D modeling technique by which the vorticity field is represented by N discrete elements of circulation Γ_j and positions $\boldsymbol{z}_j$. According to the vorticity formulation of the Navier-Stokes equation, the vorticity is simply carried with the fluid at the local velocity and it diffuses at a rate inversely proportional to the inverse of the Reynolds number, Re. It is an approach developed by many and brought to maturity by Leonard and co-workers [1, 7, 8, 9, 19, 21]. In previous numerical shear layer studies [4], researchers find that the diffusive component has little effect on global features of the roll-up and pairing dynamics. Therefore, we set $Re = \infty$ and ignore diffusion. Thus, circulation of the individual vortex elements remains constant, and their positions evolve according to the ODEs

$$\dot{\boldsymbol{z}}_j = \boldsymbol{u}(\boldsymbol{z}_j, t), \quad j \in 1, 2, 3, \ldots, n. \tag{1}$$

Here the local velocity $\boldsymbol{u}(\boldsymbol{z}_j, t)$, is given by

$$\boldsymbol{u}(\boldsymbol{z}_j, t) = \sum_{k=1,\neq j}^{N} K(\boldsymbol{z}_j, \boldsymbol{z}_k)\Gamma_k + \boldsymbol{v}(\boldsymbol{z}_j, t), \tag{2}$$

where the kernel K is the Biot-Savart law or an analogue for vortex elements of finite core size. The term $\boldsymbol{v}$ refers to the velocity due to the free stream and that induced by actuators.

2.1 Boundary Effects

For an inviscid flow the appropriate boundary condition is $\boldsymbol{u} \cdot \hat{\boldsymbol{n}} = 0$, where $\hat{\boldsymbol{n}}$ is a vector perpendicular to the boundary. We solve this exactly using image vortices and a Schwarz-Christoffel transformation. The approach is a natural choice for polygonal domains and is generally more efficient than less accurate panel methods.

We begin by finding a conformal transformation from the *physical domain* parameterized by the complex coordinate $z = x + iy$ to the upper half of the complex plane $\mathrm{Im}\{\zeta\} \geq 0$, the *transformed domain*. We represent the transformation compactly by $\zeta(z)$ and the inverse by $z(\zeta)$. According to the Schwarz-Christoffel theorem [2], one can construct the transformation by specifying its derivative:

$$\frac{dz}{d\zeta} = \frac{h}{\zeta}\left(\frac{\zeta - 1}{\zeta - h^{1/\vartheta}}\right)^{\vartheta}, \tag{3}$$

where $\vartheta = \theta/\pi$. In the Figure 2 the points $\xi_0 = 0$,

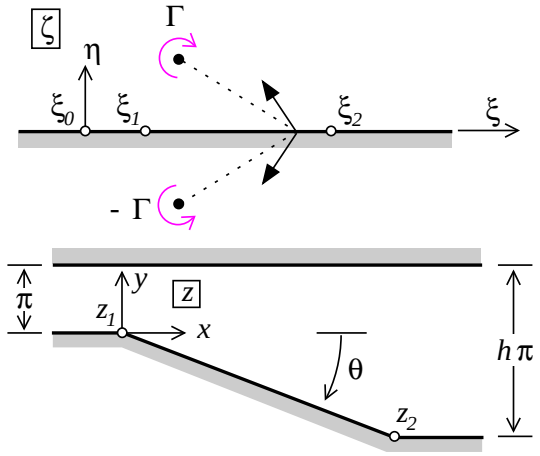

Figure 2: *Transformed and physical domains for the diffuser problem.*

$\xi_1 = 1$, and $\xi_2 = h^{1/\vartheta}$ in the transformed domain get mapped to $z_0 = -\infty$, $z_1 = 0$, and z_2 in the physical plane respectively.

Solutions to the 2-D inviscid flow problem in each of the domains map to each other through the conformal transformation and its inverse. The advantage of conformal mapping comes from the fact that boundary conditions are easily satisfied in the transformed domain. For each vortex of strength Γ_j at location ζ_j, we place an image vortex of strength $-\Gamma_j$ outside the transformed domain at $\bar{\zeta}_j$ as shown in Figure 2, where over-bar denotes complex conjugation. Via the mapping, we achieve the boundary conditions in the physical domain.

In typical vortex simulations reported in the literature (*e.g.* [20, 6, 10]) similar to this, the domain geometries are sufficiently simple that authors are able to express $\zeta(z)$ and $z(\zeta)$ explicitly in terms of elementary functions. With such problems, it is a relatively simple task to derive and integrate evolution equations for vortices in the transformed plane so they obey the proper physics in the physical domain. For the diffuser, however, we are not able to explicitly integrate (3). Therefore, we must formulate the problem so that all evaluations and integration are performed solely in the transformed domain. After simulating the evolution of the vortices for a desired amount of time, we may then determine vortex locations in the physical plane via direct numerical integration of transformation generator (3).

Within this formulation, the evolution equations for the position ζ_j of the j^{th} vortex in the transformed plane is

$$\frac{d\bar{\zeta}_j}{dt} = \frac{1}{|dz/d\zeta|^2}\left[\frac{d\tilde{\Phi}_j}{d\zeta} - \frac{i\Gamma_j}{4\pi(dz/d\zeta)}\frac{d^2z}{d\zeta^2}\right]. \quad (4)$$

Derivation is too lengthy to fit within the space constraints of this note. Here $\tilde{\Phi}_j$ is the complex velocity potential within the transformed plane of the flow induced by the free stream, actuator, all image vortices, and all vortices except the j^{th} vortex. $d\tilde{\Phi}_j/d\zeta$, therefore, gives the velocity resulting from all these elements. The factor $|dz/d\zeta|$ appearing in (4) appears due to the non-uniform scaling of the transformation as is evident in Figure 3. In the figure, a square grid is shown in

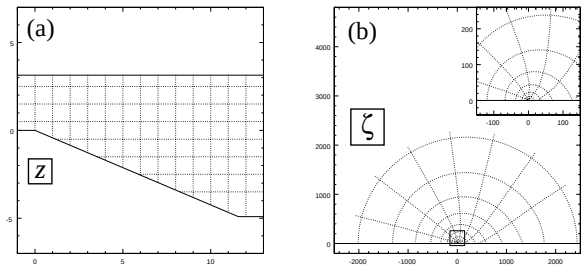

Figure 3: *A uniform square grid in the physical plane is mapped to a set of non-uniformly spaced curves in the transformed domain. The small box depicts an enlargement region.*

the physical domain along with its image in the transformed plane. The last piece in (4) is called the Routh term. It creates rotational effects around the images of the vertices which are singularities in the transformation.

2.2 Vorticity Generation

In the physical problem, flow separates from the diffuser wall at the sharp corner at the beginning of the expansion. In this inviscid setting, we recognize this phenomena as the inability of the fluid in the immediate vicinity of the corner to sustain the near-infinite acceleration necessary to abruptly change direction. The classical modeling resolution to this issue is to impose a Kutta condition [11]. It is a constraint on the degrees of freedom of the model to ensure that pressure at the sharp corner remains finite.

The standard approach to satisfy the Kutta condition in these types of problems is to introduce vorticity at each time step with position and circulation chosen to cancel the velocity at the image of the convex vertex in the transformed plane. See Figure 4. In the physical, domain, this ensures finite pressure at the corner. One difficulty in the approach is that the Kutta condition

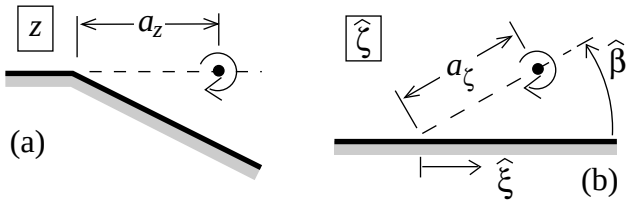

Figure 4: *Satisfaction of the Kutta condition by introduction of a vortex.*

is inherently non-unique. One can satisfy the Kutta condition by introducing a weak vortex very close to the corner, or a stronger vortex further away. This leads authors to introduce ad-hoc length scales [20, 6] and convection velocities for closure.

Instead, we adapt a variation developed by Giesing [5] which we find intellectually more satisfying. Instead of introducing a single vortex at each time step as illustrated in Figure 4, we envision a continuous sheet of vorticity of constant circulation density being formed parallel to the windward side of the corner during the course of one time step (Figure 5). In the transformed

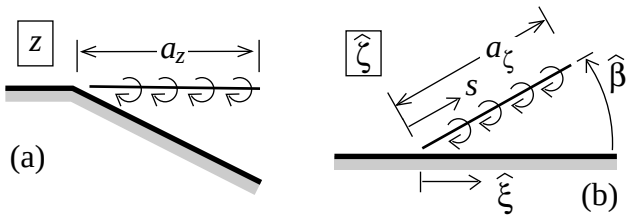

Figure 5: *An alternative formulation of the Kutta condition in which a continuous sheet of vorticity is shed during a time step.*

plane, then, the circulation density varies like s^ϑ at leading order, where s is the distance from the image of the convex corner. One then chooses the magnitude of this distribution to cancel the flow velocity at image of the corner, giving a finite velocity and finite pressure in the physical system. Conditions relating the convection velocity, sheet length, and strength must all be satisfied simultaneously. The process yields a mechanically consistent algorithm to introduce vortices that account for the separation phenomena.

2.3 Actuator Modeling

One of the goals of this modeling effort is to replicate, at least qualitatively, diffuser experiments performed by Narayanan *et al.* [16]. In the experimental effort, researchers used directed synthetic jets [13] as actuators. Schematically shown in Figure 6a, the actuator consists of a speaker placed placed in a slotted cavity. As the speaker diaphragm oscillates, fluid is sinusoidally forced through the slot near the lip of the diffuser.

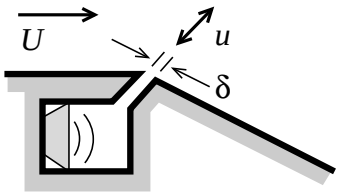

Figure 6: *Schematic representation of the actuator used in experiments performed by [16]*

To incorporate such geometry with disparate length scales into our conformal mapping formulation of the model causes numerical problems of "crowding" [22]. Thus, to avoid these difficulties, yet still represent the dominant effects of vortex sheet displacement and vorticity generation by the actuator, we propose a much simpler model. As a first cut, we simply place a point source slightly downstream of the diffuser lip. The source is depicted in both the physical and transformed domains in Figure 7.

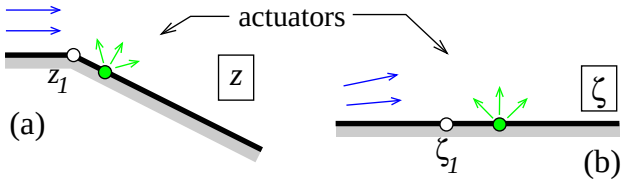

Figure 7: *Schematic representation of the actuator in the physical domain (a) and transformed domain (b) in the computational model.*

Narayanan *et al.* [16] report the peak magnitudes of the flow issuing from the actuator slot in their experiments along with c_μ, the momentum flux normalized by the momentum of the mean flow. We are able to match these quantities by appropriately choosing the location of the actuator source shown in Figure 6 and the amplitude of its sinusoidally, time-varying strength.

2.4 Vortex Merging and Removal

At each time step, the dimension of the state space increases by two: equations for the horizontal and vertical motion of each new separating vortex is introduced. To keep the problem from ballooning out of control, we also remove vortices from the simulation once they have convected sufficiently far down stream that they play a negligible role in the vortex formation and pressure recovery processes close to the separation point.

To further manage the dimension of the simulation, we allow nearby vortices sufficiently far down stream to merge. It is a strategy explored by Shiels [21] in a viscous vortex simulation of flow past a circular cylinder. The resulting merged vortex has circulation equal to the sum of the strengths of the vortices that merged and position that coincides with their center of vorticity. Whether vortices are close enough to merge is determined by their position. Figure 8 shows, for several stations along the duct, circles whose radii represent the relevant "merge distances."

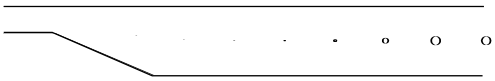

Figure 8: *Merge distances for several locations throughout the domain.*

We also remove vortices when they drift too close to the wall. Such vortices get drawn upstream due to the velocity induced by the image vortex. Such events do not occur in a viscous flow as the vortex would simply be absorbed by the boundary layer. Inviscid vortex simulation efforts typically define a boundary layer thickness, within which vortices are simply removed [20, 6].

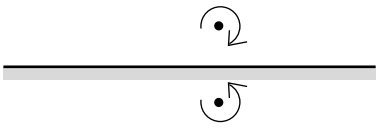

Figure 9: *Vortices close to the wall feel a strong effect from its image vortex.*

We have attempted this artificial boundary layer approach on the diffuser with only moderate success. Since vortex merging produces vortices with a wide range of strengths, it is difficult to choose a single length scale that is appropriate for all. Thus, instead of specifying an ad-hoc length, we choose to remove a vortex when it is sufficiently close to the wall that the upstream velocity induced by its image vortex is greater than free stream which tends to push the vortex down stream. The removal condition naturally scales with the strength of the vortex.

3 Results

We run the simulation with diffuser angle $\theta = 23°$ in effort to compare results with previous experiments [16, 3]. In Figure 10, we compare nondimensional pressure recovery C_p as a function of dimensionless forcing frequency or Strouhal number based on the diffuser length L.

In Figure 10a, the experimental curves are presented for three different flow speeds. In all, the optimal forcing frequency occurs roughly at $St = 0.6$. Further, the

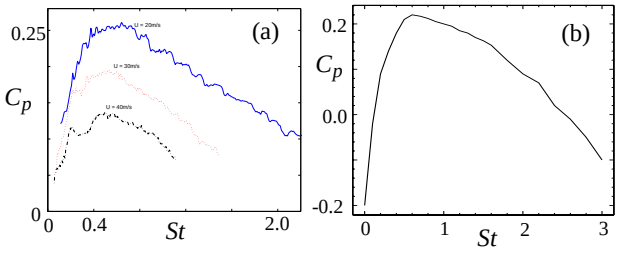

Figure 10: *Pressure recovery versus dimensionless forcing frequency for the experimental [16] system (a) and computational model (b).*

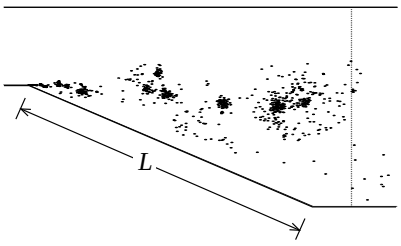

Figure 11: *Typical snapshot of vortices in uncontrolled diffuser.*

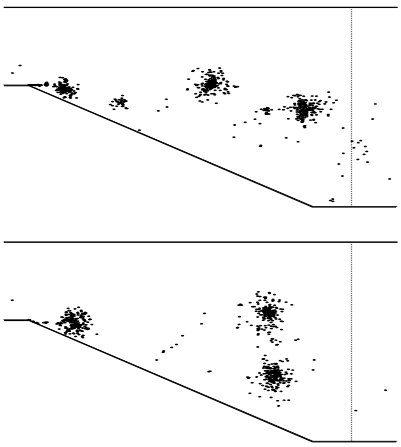

Figure 12: *Two typical snapshot of vortices in controlled diffuser at* $St = 0.6$.

shapes of the pressure recovery curves are similar indicating the week influence of Reynolds number on the physical processes that determine pressure recovery as assumed in the modeling effort. The analogous curve for the simulation is shown in Figure 10b. Although there are discrepancies in the magnitudes, the simulation correctly predicts the general form of the curve and the maximum pressure recovery at a frequency $St = 0.6$.

In Figures 11 and 12, we show typical snapshots of the vortices produced by the numerical simulation. Without any actuation (Fig. 11), we see that the flow is much less organized than when we sinusoidally force the flow at its optimal frequency (Fig. 12). In Figure 12, two successive snapshots are shown a short time apart. We observe neighboring vortices pair, creating a region of intense circulation that draws high momentum fluid of the core flow close to the wall. This is the pressure recovery mechanism we also observe in experiment as illustrated by the photograph in Figure 13 where we clearly see the smoke introduced into the core being drawn around a region of concentrated vorticity. The

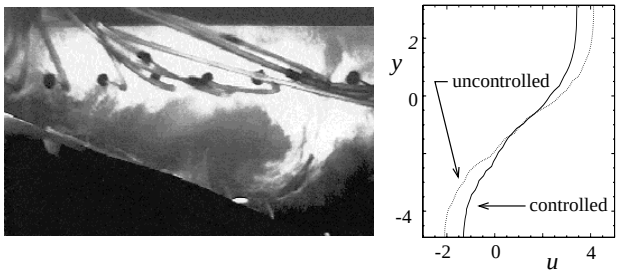

Figure 13: *Photo showing exchange of momentum in experiment with control (left). Time - averaged velocity profiles with and without control generated by computation (right).*

pairing occurs irregularly in the simulation. In an average sense, the vorticity dynamics make the velocity profile at the dotted line in Figures 11 and 12 more full as illustrated in Figure 13. Simple control volume techniques developed in [16] and reported in [3] illustrate how fuller profiles improve pressure recovery characteristics.

4 Conclusions

The simulations presented herein contain on the order of 700 vortices. Even with this coarse representation and other modeling assumptions, initial results indicate that our vortex model is capable of capturing many of the essential features of this complex dynamical system. There is still room for improvement, however, in quantitative results. The model's pressure recovery pre-

dictions are too low, and the negative values of C_p do not make physical sense. In closer examination of the vortex simulations, it appears as though the anomaly is due to vortices close to the wall artificially being carried upstream by their image vortices. While the new modeling approaches outlined in Section 2.4 has improved quantitative agreement substantially over that reported in [3] close examination of the data indicates that one should modify the artificial boundary layer to account for concentrated clusters of vorticity in addition to individual vortices.

Nonetheless, the model is very close to being a useful tool to efficiently test and synthesize new control laws without resorting to experiment or typical detailed numerical simulations which take orders of magnitude longer to run.

Acknowledgement: I wish to acknowledge fruitful discussions with Bernd Noack, Satish Narayanan, Andrezj Banaszuk, and Alex Khibnik.

References

[1] C. Chang and R. Chern. A numerical study of flow around an impulsively started circular cylinder by a deterministic vortex method. *Journal of Fluid Mechanics*, 233:243, 1991.

[2] R.V. Churchill and J.W. Brown. *Complex Variables and Applications*. McGraw Hill, 1990.

[3] B.D. Coller, B.R. Noack, S. Narayanan, A. Banaszuk, and A.I. Khibnik. Reduced-basis model for active separation control in a planar diffuser flow. *AIAA Paper 2000–2562*, 2000.

[4] A.F. Ghoniem and K.K Ng. Numerical study of the dynamics of a forced shear layer. *Physics of Fluids*, 30:706 – 721, 1987.

[5] J.P. Giesing. Vorticity and Kutta condition for unsteady multienergy flows. *Journal of Applied Mechanics*, 37:608–615, 1969.

[6] M. Kiya, K. Sasaki, and M. Arie. Discrete-vortex simulation of a turbulent separation bubble. *Journal of Fluid Mechanics*, 120:219–244, 1982.

[7] P. Koumoutsakos. *Direct Numerical Simulations of Unsteady Separated Flows Using Vortex Methods*. PhD thesis, California Institute of Technology, 1993.

[8] P. Koumoutsakos and A. Leonard. High-resolution simulations of the flow around an impulsively started cylinder using vortex methods. *Journal of Fluid Mechanics*, 296:1, 1995.

[9] P. Koumoutsakos and D. Shiels. Simulations of the viscous flow normal to an impulsively started and uniformly accelerated flat plate. *Journal of Fluid Mechanics*, 328:177, 1996.

[10] R. Krasny. Vortex sheet computations: roll-up, wakes, separation. *Lectures in Applied Mathematics*, 28:385–402, 1991.

[11] A.M. Kuethe and Y.C. Chow. *Foundations of Aerodynamics: Bases of Aerodynamic Design*. Wiley, 1986.

[12] A.H.M. Kwong and A.P. Dowling. Active boundary-layer control in diffusers. *AIAA Journal*, 32:2409–2414, 1994.

[13] D.C. McCormick. Boundary layer separation control with directed synthetic jets. In *39th AIAA Aerospace Sciences Meeting and Exhibit*, 1999.

[14] Jr. McKinzie, D.J. Turbulent boundary layer separation over a rearward facing ramp and its control through mechanical excitation. *AIAA Paper*, 91-0253, 1991.

[15] Jr. McKinzie, D.J. Delay of turbulent boundary layer detachment by mechanical excitation: Application to rearward-facing ramp. Technical Report 3541, NASA Technical Paper, 1996.

[16] S. Narayanan, B.R. Noack, A. Banaszuk, and A.I. Khibnik. Dynamic flow separation control in a low-speed planar diffuser. Technical Report R99-1.910.9901-4.1, United Technologies Research Center, 1999.

[17] B. Nishri and I. Wygnanski. Effects of periodic excitation on turbulent flow separation from a flap. *AIAA Journal*, 36(4):547–556, 1998.

[18] D.E. Parekh and Glezer A. Avia: Adaptive virtual aerosurface. *AIAA Paper 2000–2474*, 2000.

[19] F. Pepin. *Simulation of the Flow Past an Impulsively Started Cylinder Using a Discrete Vortex Method*. PhD thesis, California Institute of Technology, 1990.

[20] T. Sarpkaya. An inviscid model of two-dimensional vortex shedding for transient and asymptotically steady separated flow over an inclined plate. *Journal of Fluid Mechanics*, 68:109–128, 1975.

[21] D. Shiels. *Simulation of Controlled Bluff Body Flow with a Viscous Vortex Method*. PhD thesis, California Institute of Technology, 1998.

[22] L.N. Trefethen. Numerical computation of the schwarz-christoffel transformation. *SIAM J. Sci. Stat. Comput.*, 1, 1980.

[23] H. Viets, M. Piatt, and M. Ball. Forced vortices near a wall. *AIAA Paper 81–0256*, 1981.